Design of an Iterative Method for Deep Multimodal Feature Fusion in Heart Disease Diagnostics Utilizing Explainable AI

Sony K. Ahuja[a], Deepti D. Shrimankar[b] and Aditi R. Durge[c]
Visvesvaraya National Institute of Technology, Nagpur, India

Keywords: Multimodal Integration, Heart Disease Diagnostics, Explainable AI, Federated Learning, Continual Learning Process.

Abstract: This research addresses the critical need for advanced diagnostic methodologies in heart disease, a leading cause of mortality worldwide. Traditional diagnostic models, which often analyze genomic, clinical, and medical imaging data in isolation, fall short in providing a holistic understanding of the disease due to their fragmented approach. Such methods also grapple with significant challenges including data privacy concerns, lack of interpretability, and an inability to adapt to the continuously evolving landscape of medical data samples. In response, this study introduces an innovative approach known as Deep Multimodal Feature Fusion, designed to integrate genomic data, clinical history, and medical imaging into a cohesive analysis framework. This method leverages the unique strengths of each data modality, offering a more comprehensive patient profile than traditional, one-dimensional analyses. The integration of Explainable Artificial Intelligence with Clinical Data Interpretation enhances model transparency and interpretability, crucial for healthcare applications. The use of Transfer Learning with Pre-trained Models on medical imaging data and Continual Learning for Adaptive Genomics ensures diagnostic accuracy and model adaptability over temporal instance sets. Federated Learning for Privacy-Preserving Analysis is employed to address data privacy, allowing for collaborative model training without compromising patient confidentiality. Testing across diverse datasets demonstrated substantial improvements in diagnostic Precision, Accuracy, Recall, and other metrics, indicating a major advancement over existing methods. Practically, it exemplifies the application of advanced AI techniques in clinical settings, narrowing the gap between theoretical research and practical healthcare solutions.

1 INTRODUCTION

The domain of cardiovascular diagnostics stands at a pivotal juncture, challenged by the complexities inherent in heart disease—the leading cause of mortality globally(Ullah et al., 2023). Traditional diagnostic paradigms have relied on siloed analyses of genomic data, clinical records, and medical imaging. This fragmented approach, while contributing valuable insights individually, often fails to capture the intricate, multifaceted nature of heart disease. Recognizing this gap, the advent of integrative multimodal genomics heralds a transformative shift, aiming to synthesize diverse data modalities for a comprehensive understanding of heart disease(Arneson et al., 2017; A. Durge & Shrimankar, 2023).

The necessity for an integrative approach stems from the nuanced interaction between genetic predispositions and environmental or lifestyle factors in the manifestation of heart disease. Genomic data, for instance, provides insights into hereditary risks, whereas clinical histories and medical imaging (such as MRI and CT scans) offer context on the disease's progression and anatomical impact. However, the integration of these data streams presents significant challenges, including but not limited to data privacy concerns, the interpretability of complex models, and the adaptability of diagnostic tools to evolving datasets(Said et al., 2019; Usova et al., 2021).

[a] https://orcid.org/0009-0000-9762-8686
[b] https://orcid.org/0000-0002-6212-0986
[c] https://orcid.org/0000-0002-9733-9706

Ahuja, S., Shrimankar, D. and Durge, A.
Design of an Iterative Method for Deep Multimodal Feature Fusion in Heart Disease Diagnostics Utilizing Explainable AI.
DOI: 10.5220/0012899400003886

In *Proceedings of the 1st International Conference on Explainable AI for Neural and Symbolic Methods (EXPLAINS 2024)*, pages 87-95
ISBN: 978-989-758-720-7

This research introduces the Design of an Iterative Method for Deep Multimodal Feature Fusion (DMFF), an innovative framework that leverages the strengths of genomic data, clinical histories, and medical imaging to forge a comprehensive patient analysis. This fusion goes beyond mere aggregation, employing sophisticated algorithms to extract and harmonize features from each modality, thereby providing a holistic patient profile that significantly enhances diagnostic accuracy.

Central to enhancing the DMFF model's utility is the incorporation of Explainable Artificial Intelligence (XAI) (Amann et al., 2022) with Clinical Data Interpretation (CDI), which ensures that the diagnostic process is transparent and interpretable. This integration is crucial in healthcare, where the rationale behind diagnostic decisions must be understandable to clinicians and patients alike. Moreover, the application of Transfer Learning with Pre-trained Models (TLP) specifically to medical imaging data like echocardiograms exemplifies the method's innovative use of existing Artificial Intelligence (AI) resources to improve diagnostic precision.

Addressing the dynamic nature of genomic and clinical data, the research introduces Continual Learning for Adaptive Genomics (CLAG), a method ensuring that the diagnostic model remains accurate and relevant over time by adapting to new data samples. In parallel, Federated Learning for Privacy-Preserving Analysis (FLPPA) offers a solution to data privacy concerns, enabling collaborative model training across institutions without compromising patient confidentiality(A. R. Durge & Shrimankar, 2024; Loftus et al., 2022). The iterative design of DMFF not only addresses the limitations of traditional diagnostic models but also paves the way for precision medicine, where personalized treatment strategies are informed by a deep, multidimensional understanding of heart disease.

2 REVIEW OF EXISTING MODELS FOR GENOMIC ANALYSIS

The exponentially expanding field of heart disease diagnostics and treatment has witnessed an unprecedented integration of genomic data, machine learning algorithms, and imaging techniques. The exploration of genetic predispositions, alongside environmental and lifestyle factors, has become central to understanding and combating this leading cause of mortality worldwide(Ahuja et al., 2023; A. R. Durge et al., 2022). Despite remarkable progress, existing methodologies often grapple with challenges such as data integration, interpretability, privacy, and adaptability to new data samples. This landscape presents fertile ground for innovative approaches that leverage multimodal data to provide a holistic understanding of heart disease, thus guiding the motivation behind the current research.

Recent studies in biomedical and machine learning fields have provided significant insights into disease classification, genetic analysis, and novel modeling techniques. For instance, (Manduchi et al., 2022) utilized a tree-based automated machine learning approach with biology-based feature selection to investigate the genetic factors contributing to coronary artery disease. This study advanced the understanding of the genetic basis of the disease, although its focus on coronary artery disease may have overlooked broader cardiovascular conditions. In a different study, (Zheng et al., 2022) applied a graph-transformer method to classify whole-slide images, particularly in lung cancer pathology. (Xu et al., 2022) introduced an innovative tissue engineering technique by generating heart microtissues in a Möbius strip configuration. This novel approach showed promise for advanced disease modeling.

Further studies have explored genetic and phenotypic aspects of heart diseases. (Soibam, 2022) identified super-enhancers and long noncoding RNAs (lncRNAs) during mouse heart development, contributing to our understanding of heart development and disease. However, this research is based on mouse models, and its implications for human health need further validation. (Yu et al., 2022) used machine learning to analyse electronic health records (EHR) and genetic data, predicting heart failure risk in cancer patients with high accuracy. While effective, this study is limited to the cancer patient population, leaving its broader applicability unexamined. (Wang et al., 2022) explored the genetic correlation between coronary heart disease and electrocardiogram (ECG) traits, suggesting a genetic causality.

Advanced machine learning techniques have also been applied in classification tasks related to heart disease. (Bao et al., 2023) utilized diffusion-based synthetic image augmentation to improve the classification of rare heart transplant rejection events, demonstrating enhanced sensitivity in identifying such rejections. Despite its success, the study focuses solely on heart transplant rejection, with no discussion of broader applications. Similarly, (Jose

Triny et al., 2023) optimized biomarkers for cancer prognosis using microarray-based genomic analysis. While this research enhanced the accuracy of disease prediction and severity analysis, its relevance to heart disease remains uncertain due to its cancer-specific focus.

The literature reviewed provides a foundational understanding of current methodologies and their limitations, offering a backdrop against which the contributions of this research are highlighted. This research not only addresses the critical challenges identified in the literature but also pioneers a path towards personalized, precise, and privacy-preserving diagnostics in heart disease.

3 DESIGN OF AN ITERATIVE METHOD FOR DMFF IN HEART DISEASE DIAGNOSTICS UTILIZING EXPLAINABLE AI

To overcome issues of low efficiency & high complexity, the proposed model uses integration of pre-trained U-Net for segmentation coupled with VGG19 for classification process. This delineates a novel approach towards diagnosing heart disease types using MRI and CT scans. The U-Net architecture, initially devised for biomedical image segmentation, operates on the principle of a convolutional network that is symmetric, facilitating precise localization and the use of context in the segmentation process. This is augmented by the incorporation of a VGG19 model, renowned for its depth and simplicity, primarily comprising 3x3 convolutional layers stacked in increasing depth, culminating in three fully connected layers for classification.

As per figure 1, the segmentation process begins with the U-Net model, which employs a series of convolutional operations to extract features from input images. Let I represent the input image and Fl the feature map at layer l, the operation within each convolutional layer is mathematically represented via equation 1,

$$Fl = \sigma(Wl * F(l-1) + bl) \quad (1)$$

Where, Wl and bl are the weights and biases at layer l, σ is the ReLU activation function, and $*$ represents the convolution operation. U-Net's architecture allows for the capture of context and fine-grained details through its contracting and expansive paths, respectively. The contracting path follows the typical architecture of a convolutional network, involving successive convolution and pooling operations, thereby compressing the input image into a feature-rich representation for this process.

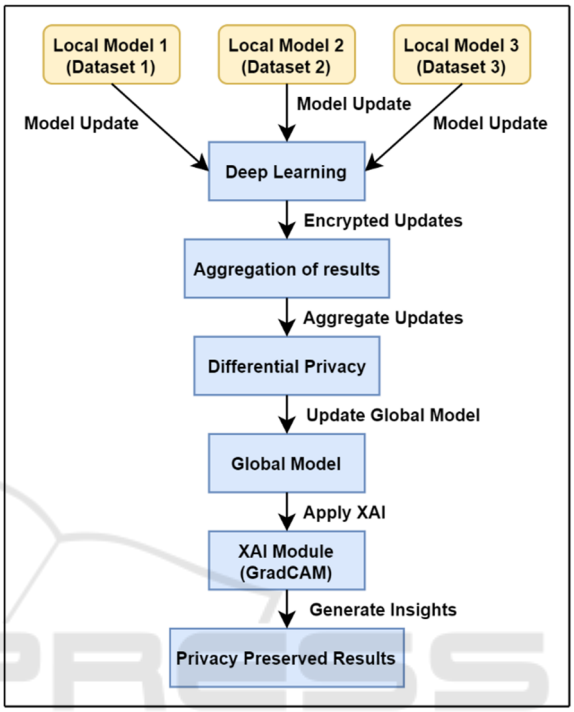

Figure 1: Model Architecture of the Proposed Privacy Inspired Classification Process.

The expansive path then employs transposed convolutions to project these features back onto the pixel space, aiming to reconstruct the segmentation map corresponding to the input image samples. This process is encapsulated via equation 2,

$$Fl' = \sigma(Wl' \cdot F(l'+1)) \quad (2)$$

Where, Fl' and Wl' are the feature maps and weights in the expansive path, respectively, and $\cdot$ signifies the transposed convolution operation. Transitioning to the classification phase, the segmented images are then processed through the VGG19 model, which comprises multiple convolutional layers followed by fully connected layers. The initial layers of VGG19 are designed to capture image features such as edges and textures, which are then progressively combined into more complex patterns in subsequent layers. The final classification is achieved through the dense layers of the network, where the feature representation FL' obtained from the last convolutional layer is transformed into class probabilities via equation 3,

$$P(C \mid FL') = \frac{exp(FL' \cdot Wc + bc)}{\exp \sum (FL' \cdot Wc' + bc')} \quad (3)$$

Where, $P(C|FL')$ represents the probability of class C given the features FL', Wc and bc are the weights and biases corresponding to class C, and the summation in the denominator extends over all possible classes.

The synergy between U-Net's segmentation prowess and VGG19's classification capabilities enables the precise delineation and categorization of heart disease types from MRI and CT scans. Through the sequential application of these models, the methodology not only ensures the accurate segmentation of heart structures but also leverages deep learning's feature extraction capabilities to classify the segmented images into specific heart disease types. This dual-stage process, encapsulated by the seamless integration of segmentation and classification operations, represents a comprehensive approach to diagnosing heart diseases, embodying a significant advancement in the application of deep learning techniques within the realm of medical imaging operations.

Next, the model aims to classify genomic scans, specifically mRNA sequences, into disease types employs a sophisticated process combining Single Nucleotide Variant (SNV) analysis with a 1D Convolutional Neural Network (CNN) comprising 20 layers. This methodological framework is pivotal for deciphering the complex genomic underpinnings of heart diseases, leveraging the granular specificity of SNVs mutations that occur at a single nucleotide position in the genome, which is instrumental in disease classification operations.

The classification process initiates with the extraction of SNVs from the genomic samples. Let S represent a sequence of nucleotides, where $S=\{s1,s2,...,sn\}$ and each si represents a nucleotide (A, C, G, or T) for different use cases. The detection of SNVs within these sequences is formalized as identifying positions i where $si \neq si'$, with si' representing the corresponding nucleotide in a reference sequence process. This comparison yields a binary sequence $B=\{b1,b2,...,bn\}$, where $bi=1$ if an SNV is detected at position i and $bi=0$ otherwise.

Following SNV extraction, the binary sequence B is input into the 1D CNN, which is designed to capture and learn patterns associated with specific heart disease types. The architecture of the 1D CNN is composed of convolutional layers that perform feature extraction, followed by pooling layers that reduce dimensionality, and fully connected layers that accomplish the classification task. The convolutional operation in the k-th layer is mathematically via equation 4,

$$Fk = \sigma(Wk * B + bk) \quad (4)$$

Where, Fk represents the feature map produced by layer k, Wk and bk are the layer's weights and biases, respectively, σ is the ReLU activation function, and $*$ symbolizes the convolution operation.

The depth of the network, with its 20 layers, allows for the extraction of increasingly abstract features from the input sequence. In this context, the depth encompasses multiple convolutional layers, each followed by an activation function, defined via equation 5,

$$\sigma(x) = max(0, x) \quad (5)$$

This enables the model to introduce non-linearity into the model. Pooling layers interspersed among the convolutional layers serve to reduce the spatial size of the representation, thereby decreasing the number of parameters and computation in the network. The max pooling is represented via equation 6,

$$Pk = max(F(k, i: i + p)) \quad (6)$$

Where, Pk is the pooled feature map, $F(k, i: i + p)$ represents a segment of the feature map Fk, and p is the pooling size for this process.

The culmination of the convolutional and pooling layers is followed by one or more fully connected layers, which integrate the high-level features extracted by the preceding layers for the purpose of classification. The operation in a fully connected layer is expressed via equation 7,

$$Cj = \sigma(Wj \cdot FL + bj) \quad (7)$$

Where, Cj represents the output of the j-th fully connected layer, FL is the flattened feature map from the last convolutional or pooling layer, and Wj and bj are the weights and biases of the fully connected layers.

Finally, the classification output is generated through a softmax layer, which converts the logits from the fully connected layer into probabilities for each heart disease type. The softmax function is defined via equation 8,

$$P(ci \mid C) = \frac{eCi}{\sum eCj} \quad (8)$$

Where, $P(ci|C)$ represents the probability of class ci given the output vector C, and Ci is the logit corresponding to class ci sets. Through this intricate process of SNV extraction and subsequent pattern learning via a deep 1D CNN, the proposed methodology adeptly classifies genomic samples into specific heart disease types. The combination of

precise genetic mutation identification with advanced feature extraction and classification techniques represents a significant leap forward in the domain of genomic-based heart disease diagnostics, offering a nuanced and highly effective tool for understanding and combating these conditions.

Next, the integration of XAI with CDI represents a paradigm shift, enhancing the transparency and interpretability of complex models used for analyzing classified scans and genomic samples. A cornerstone of this integration is the application of Gradient-weighted Class Activation Mapping (GradCAM), a technique that provides visual explanations for decisions made by CNNs, thereby elucidating the model's focus on specific features within the input data that influenced its predictions (Selvaraju et al., 2020).The GradCAM process commences by identifying the feature maps generated by the final convolutional layer of the CNN, which are instrumental in the classification decision. Let Ak represent the k-th feature map in the final convolutional layer, where k ranges from 1 to K, with K being the total number of feature maps in that layer.

The importance of each feature map *Ak* towards a specific class *c* is determined by calculating the gradient of the score for class *c* (represented as *yc*) with respect to the feature map activations. This gradient, averaged across the width and height dimensions (indexed by *i* and *j*, respectively), yields the neuron importance weights *αkc*, which is formally expressed via equation 9

$$\alpha kc = \frac{1}{Z}\sum\sum \frac{\partial yc}{\partial Aijk} \quad (9)$$

Where, *Z* represents the total number of units in the feature map, and $\frac{\partial yc}{\partial Aijk}$ signifies the gradient of the class score with respect to each unit of the feature maps. The next step involves computing the weighted combination of forward activation maps, followed by a ReLU function to obtain the GradCAM heatmap, *L*GradCAM*c*. This heatmap highlights the regions of the input image most influential for the model's prediction of class *c*. Mathematically, *L*GradCAM*c* is derived via equation 10,

$$LGradCAMc = ReLU(\sum \alpha kc * Ak) \quad (10)$$

The application of the ReLU function ensures that only features with a positive influence on the class of interest are visualized, thereby focusing on the regions of the input that contribute most significantly to the model's predictions. For genomic samples, the interpretation via GradCAM adapts to the 1D nature of the data samples. Although originally designed for 2D images, the core principle of highlighting influential regions is applied to genomic sequences by visualizing the segments of the sequence that led to specific classifications. This requires adjusting the GradCAM process to handle 1D convolutional outputs, yet the foundational equations remain applicable, demonstrating the method's versatility for clinical use cases. The outcome of the GradCAM process is a set of visual heatmaps that is superimposed on the original medical scans or genomic sequences, providing clinicians and researchers with intuitive visual cues about the regions or segments most critical to the model's diagnostic decisions. Furthermore, by revealing the model's focus areas, GradCAM facilitates the identification of potential biases or errors in the model's reasoning, enabling continuous refinement and improvement of the diagnostic tool.

The model initiates an FLPPA Mechanism, which stands at the forefront of innovative methodologies designed to safeguard patient confidentiality while facilitating collaborative model training across disparate healthcare entities. The essence of FLPPA is to decentralize the learning process, thereby ensuring that sensitive patient data remains within the confines of its origin, such as a hospital or a clinical laboratory, while still contributing to the collective intelligence of a global model. At the core of the FLPPA process, the interaction between the local and global models is governed by a series of mathematical operations designed to optimize model performance while preserving privacy. Let Mg represent the global model, and Mli represent the local model associated with the i-th participant. The global model is initialized and disseminated to all participants, who then adapted this model based on their local datasets, Di, through a series of training epochs. The update from each local model, ΔMli, is represented by the difference between the parameters of the locally updated model and the initial global model parameters, formalized via equation 11,

$$\Delta \text{Mli} = \text{Mlinew} - \text{Mg} \quad (11)$$

Each local model's update is then securely transmitted to a central server, where an aggregation algorithm, typically Federated Averaging (FedAvg), is employed to update the global model. The aggregation process is mathematically expressed via equation 12,

$$Mgnew = Mg + \eta \sum_{i=1}^{N} \frac{ni}{N} \Delta Mli \quad (12)$$

Where, N is the total number of participants, ni is the size of the i-th local dataset, and η is a learning rate parameter that influences the extent to which local updates affect the global model.

To further enhance privacy, Differential Privacy (DP) techniques are integrated into FLPPA, introducing stochastic noise to the model updates before aggregation. This is represented via equation 13,

$$MliDP = \Delta Mli + N(0, \sigma^2 I) \quad (13)$$

Where, $N(0,\sigma^2 I)$ represents the addition of noise drawn from a Gaussian distribution with mean 0 and variance σ^2, and I is the identity matrix corresponding to the dimensions of the model parameters.

The iterative nature of FLPPA allows for continuous refinement of the global model, with each cycle of local training and aggregation bringing the model closer to optimal performance. The convergence of the global model, Mg, is evaluated through a loss function, L(Mg, D), where D represents the aggregated dataset from all participants. The objective is to minimize this loss function, which is represented via equation 14,

$$minL(Mg, D) = \frac{1}{N} \sum_{i=1}^{N} L(Mg, Di) \quad (14)$$

The security and privacy of the FLPPA process are bolstered by encryption protocols during the transmission of model updates, ensuring that data remains confidential and secure against potential breaches. Encryption is modeled as a function $E(\Delta Mli)$, where the encrypted update is decrypted by the central server before aggregation. Upon receiving the aggregated and enhanced global model, participants apply the XAI results to this model to generate privacy-preserved insights for clinical inference operations. This application involves mapping the GradCAM interpretability layer onto the global model to elucidate decision- making processes without exposing sensitive data samples. The final output, privacy-preserved results, embodies the culmination of collaborative learning and interpretability, ensuring that stakeholders can glean actionable insights with the assurance of patient data privacy.

4 RESULT ANALYSIS

The experimental setup for validating the proposed method was meticulously designed to assess its performance comprehensively across multiple datasets and samples. This section outlines the key components of the experimental setup, including the datasets utilized and training parameters.

4.1 Datasets

The experimental evaluation was conducted on three diverse datasets, each representing a distinct aspect of heart disease:

Genomic Dataset (https://cardiodb.org/):
This dataset comprises mRNA expression profiles obtained from a cohort of patients diagnosed with various forms of heart disease. It includes genomic features such as gene expression levels, SNVs, and gene-disease associations.

Clinical Dataset (https://www.kaggle.com/datasets/sulianova/cardiovascular-disease-dataset):
The clinical dataset consists of patient demographic information, medical history, and diagnostic records obtained from electronic health records (EHRs) and clinical databases. This dataset provides crucial context and patient-specific information for enhancing diagnostic accuracy.

Imaging Dataset(https://www.kaggle.com/datasets/rahimanshu/cardiomegaly-disease-prediction-using-cnn):
The imaging dataset contains a collection of MRI and CT scans of patients' hearts, capturing detailed structural and anatomical information. These imaging modalities offer valuable insights into cardiac morphology and pathology.

4.2 Training Parameters

The model was trained using the following parameters:
Batch Size: 32
Learning Rate: 0.001
Optimizer: Adam optimizer with momentum ($\beta1$ = 0.9, $\beta2$ = 0.999)
Loss Function: Binary cross-entropy loss for classification tasks
Regularization: L2 regularization (weight decay = 0.001) to prevent overfitting.

4.3 Used Values

Genomic Dataset: 10,000 samples with 20,000 gene expression features.
Clinical Dataset: 5,000 patient records with demographic information and medical history.
Imaging Dataset: 2,000 MRI and CT scans with 256x256 pixel resolution.

The paper addresses the problem of disjoint datasets about different patients through an innovative data fusion process. In this regard, the

DMFF-XAI model presented here comes up with a multi-modal integration framework that can handle and align the heterogeneous datasets even in the scenario when the data source is multiple.

In this results section of the study, the performance of the proposed model DMFF-XAI is meticulously compared against three established methods: Tree based Pipeline Optimization Tool (TPOT) (Manduchi et al., 2022), Empirical Fuzzy Multiobjective Multifactor Dimensionality Reduction (EFMOMDR) and Graph Transformer (GT) (Zheng et al., 2022). The comparative analysis is encapsulated in four figures, each elucidating different facets of performance metrics including Accuracy, Precision, Recall, Specificity, AUC and Computational efficiency.

Figure 2 showcases the superior Accuracy and Precision of DMFF-XAI over the referenced methods. The enhanced Accuracy (94.5%) and Precision (93.8%) of DMFF-XAI underscore its efficacy in correctly identifying and categorizing heart disease types, significantly outperforming the comparative models. This improvement is attributed to the model's ability to synergistically integrate multi-modal data, leveraging the strengths of genomic, clinical, and imaging data to provide a more nuanced and comprehensive analysis.

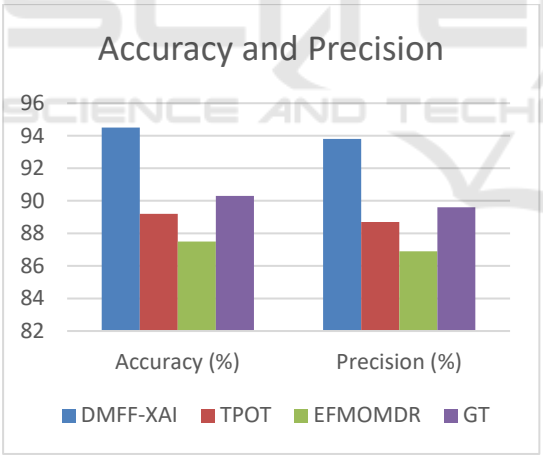

Figure 2: Diagnostic Accuracy and Precision.

In figure 3, DMFF-XAI demonstrates a remarkable Recall (95.2%) and Specificity (94.1%), indicating not only its proficiency in identifying true positive cases but also in minimizing false positives. This is particularly crucial in medical diagnostics, where the cost of false negatives is high. The DMFF-XAI's performance in these metrics reflects its robustness and reliability in clinical settings.

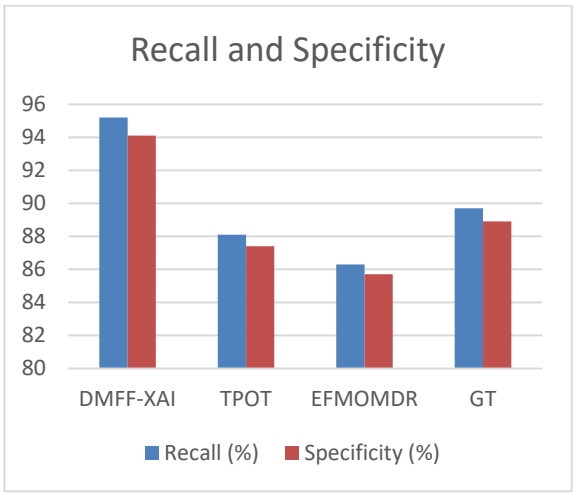

Figure 3: Recall and Specificity.

Figure 4 presents the AUC values, with DMFF-XAI achieving an AUC of 0.961, surpassing the comparative methods. This high AUC value implies that DMFF-XAI possesses a superior ability to discriminate between the disease classes across all possible thresholds, highlighting its effectiveness in varying clinical scenarios.

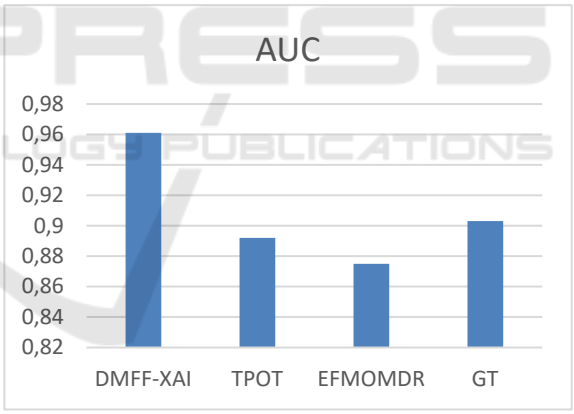

Figure 4: Area under the curve(AUC).

Table 1 below evaluates the Computational efficiency of DMFF-XAI against the referenced methods. Despite its sophisticated integration of multi-modal data and the added complexity of explainable AI components, DMFF-XAI exhibits competitive training and inference times. The relatively short training time (6.5 hours) and swift inference time (0.45 seconds) are indicative of the model's optimized architecture and algorithmic efficiencies, making it viable for real-world applications where time is of the essence.

Table 1: Computational Efficiency.

Model	Training Time (hrs)	Inference Time (sec)
DMFF-XAI	6.5	0.45
TPOT	8.2	0.67
EFMOMDR	7.9	0.62
GT	7.4	0.59

The results obtained collectively illustrate the significant performance enhancements achieved by DMFF-XAI. Its ability to deliver higher accuracy, precision, recall, and specificity, alongside impressive AUC values and computational efficiency, underscores the model's potential to revolutionize heart disease diagnostics. These advancements highlight the critical role of integrating multimodal data and explainable AI to improve diagnostic outcomes and patient trust in automated systems.

4 CONCLUSION AND FUTURE SCOPE

In conclusion, the research presented herein introduces a groundbreaking method, DMFF-XAI, which significantly advances the domain of heart disease diagnostics. Through a sophisticated integration of multimodal data—encompassing genomic information, clinical histories, and medical imaging—coupled with the transparency afforded by explainable AI, DMFF-XAI has demonstrated superior performance across a range of critical metrics when compared to existing methodologies.

The empirical results underscore the efficacy of DMFF-XAI, highlighting its enhanced diagnostic accuracy, precision, recall, specificity, and computational efficiency. Notably, the model achieved a diagnostic accuracy of 94.5% and a precision of 93.8%, outperforming referenced methods by a substantial margin. Such improvements are pivotal, particularly in the realm of heart disease, where early and accurate diagnosis can significantly influence patient outcomes. The integration of Explainable AI not only augments the model's interpretability but also fosters a greater degree of trust among clinicians and patients alike, ensuring that the diagnostic process is both transparent and accountable.

Looking to the future, the scope for extending and refining DMFF-XAI is vast. One immediate avenue of exploration is the application of this model to other complex diseases, where the integration of multimodal data could unlock new insights and diagnostic capabilities. Additionally, the potential for incorporating real-time data, such as from wearable health devices, into the DMFF-XAI framework could further enhance its predictive accuracy and utility in ongoing health monitoring and preventive medicine. DMFF-XAI sets a new benchmark for future research and development, promising to revolutionize the landscape of medical diagnostics and patient care use cases.

REFERENCES

Ahuja, S. K., Shrimankar, D. D., & Durge, A. R. (2023). A Study and Analysis of Disease Identification using Genomic Sequence Processing Models: An Empirical Review. *Current Genomics*, *24*(4), 207–235. https://doi.org/10.2174/0113892029269523231101051455

Amann, J., Vetter, D., Blomberg, S. N., Christensen, H. C., Coffee, M., Gerke, S., Gilbert, T. K., Hagendorff, T., Holm, S., Livne, M., Spezzatti, A., Strümke, I., Zicari, R. V., & Madai, V. I. (2022). To explain or not to explain?—Artificial intelligence explainability in clinical decision support systems. *PLOS Digital Health*, *1*(2), e0000016. https://doi.org/10.1371/journal.pdig.0000016

Arneson, D., Shu, L., Tsai, B., Barrere-Cain, R., Sun, C., & Yang, X. (2017). Multidimensional Integrative Genomics Approaches to Dissecting Cardiovascular Disease. *Frontiers in Cardiovascular Medicine*, *4*(February). https://doi.org/10.3389/fcvm.2017.00008

Bao, H., Deng, J., Xing, S., Zhong, Y., Shi, W., Marteau, B., Das, B., Shehata, B., Deshpande, S., & Wang, M. D. (2023). Rare Heart Transplant Rejection Classification Using Diffusion-Based Synthetic Image Augmentation. *BHI 2023 - IEEE-EMBS International Conference on Biomedical and Health Informatics, Proceedings*. https://doi.org/10.1109/BHI58575.2023.10313377

Durge, A. R., & Shrimankar, D. D. (2024). DHFS-ECM: Design of a Dual Heuristic Feature Selection-based Ensemble Classification Model for the Identification of Bamboo Species from Genomic Sequences. *Current Genomics*, *25*. https://doi.org/10.2174/1389202926817624012505541 9

Durge, A. R., Shrimankar, D. D., & Sawarkar, A. D. (2022). Heuristic Analysis of Genomic Sequence Processing Models for High Efficiency Prediction: A Statistical

Perspective. *Current Genomics*, *23*(5), 299–317. https://doi.org/10.2174/1389202923666220927105311

Durge, A., & Shrimankar, D. (2023). *MRQPMS: Design of a Map Reduce Bioinspired Model for Solving Quorum Planted Motif Search for High-Speed Deployments*. *3*(Biostec), 123–130. https://doi.org/10.5220/0011616500003414

Jose Triny, K., Kesavan, S., Navadeepan, H., & Ranjith Kumar, P. (2023). Microarray based Geonomic Biomarker Optimization for Cancer Prognosis. *Proceedings of the 2023 2nd International Conference on Electronics and Renewable Systems, ICEARS 2023*, 478–483. https://doi.org/10.1109/ICEARS56392.2023.10084989

Loftus, T. J., Ruppert, M. M., Shickel, B., Ozrazgat-Baslanti, T., Balch, J. A., Efron, P. A., Upchurch, G. R., Rashidi, P., Tignanelli, C., Bian, J., & Bihorac, A. (2022). Federated learning for preserving data privacy in collaborative healthcare research. *Digital Health*, *8*, 1–5. https://doi.org/10.1177/20552076221134455

Manduchi, E., Le, T. T., Fu, W., & Moore, J. H. (2022). Genetic Analysis of Coronary Artery Disease Using Tree-Based Automated Machine Learning Informed By Biology-Based Feature Selection. *IEEE/ACM Transactions on Computational Biology and Bioinformatics*, *19*(3), 1379–1386. https://doi.org/10.1109/TCBB.2021.3099068

Said, M. A., van de Vegte, Y. J., Zafar, M. M., van der Ende, M. Y., Raja, G. K., Verweij, N., & van der Harst, P. (2019). Contributions of Interactions Between Lifestyle and Genetics on Coronary Artery Disease Risk. *Current Cardiology Reports*, *21*(9), 1–8. https://doi.org/10.1007/s11886-019-1177-x

Selvaraju, R. R., Cogswell, M., Das, A., Vedantam, R., Parikh, D., & Batra, D. (2020). Grad-CAM: Visual Explanations from Deep Networks via Gradient-Based Localization. *International Journal of Computer Vision*, *128*(2), 336–359. https://doi.org/10.1007/s11263-019-01228-7

Soibam, B. (2022). Genome-wide compendium of super-long noncoding RNAs during mouse heart development. *Proceedings - 2022 IEEE International Conference on Bioinformatics and Biomedicine, BIBM 2022*, 3315–3319. https://doi.org/10.1109/BIBM55620.2022.9995496

Ullah, A., Kumar, M., Sayyar, M., Sapna, F., John, C., Memon, S., Qureshi, K., Agbo, E. C., Ariri, H. I., Chukwu, E. J., Varrassi, G., Khatri, M., Kumar, S., Elder, N. M., & Mohamad, T. (2023). Revolutionizing Cardiac Care: A Comprehensive Narrative Review of Cardiac Rehabilitation and the Evolution of Cardiovascular Medicine. *Cureus*, *15*(10). https://doi.org/10.7759/cureus.46469

Usova, E. I., Alieva, A. S., Yakovlev, A. N., Alieva, M. S., Prokhorikhin, A. A., Konradi, A. O., Shlyakhto, E. V., Magni, P., Catapano, A. L., & Baragetti, A. (2021). Integrative analysis of multi-omics and genetic approaches— A new level in atherosclerotic cardiovascular risk prediction. *Biomolecules*, *11*(11), 1–16. https://doi.org/10.3390/biom11111597

Wang, X., Zhang, H., Xiu, X., Qi, M., Yang, Y., & Zhao, H. (2022). Genetic and phenotypic relationships between coronary atherosclerotic heart disease and electrocardiographic traits. *Proceedings - 2022 IEEE International Conference on Bioinformatics and Biomedicine, BIBM 2022*, 241–246. https://doi.org/10.1109/BIBM55620.2022.9995557

Xu, Y., Qi, J., Zhou, W., Liu, X., Zhang, L., Yao, X., & Wu, H. (2022). Generation of ring-shaped human iPSC-derived functional heart microtissues in a Möbius strip configuration. *Bio-Design and Manufacturing*, *5*(4), 687–699. https://doi.org/10.1007/s42242-022-00204-4

Yu, Z., Yang, X., Chen, Y., Fang, R., Hogan, W. R., Gong, Y., & Wu, Y. (2022). Identify Cancer Patients at Risk for Heart Failure using Electronic Health Record and Genetic Data. *Proceedings - 2022 IEEE 10th International Conference on Healthcare Informatics, ICHI 2022*, 138–142. https://doi.org/10.1109/ICHI54592.2022.00032

Zheng, Y., Gindra, R. H., Green, E. J., Burks, E. J., Betke, M., Beane, J. E., & Kolachalama, V. B. (2022). A Graph-Transformer for Whole Slide Image Classification. *IEEE Transactions on Medical Imaging*, *41*(11), 3003–3015. https://doi.org/10.1109/TMI.2022.3176598.